Desalination and Water Treatment
www.deswater.com

doi:10.5004/dwt.2017.21324

87 (2017) 222–232
August

Study of a polyether-based carboxylate inhibiting $CaSO_4 \cdot 2H_2O$ and $CaCO_3$ in cooling water system

Jun Li[a], Yuming Zhou[a,*], Qingzhao Yao[a,*], Tiantian Wang[a], Ao Zhang[a], Yiyi Chen[a], Qiuli Nan[b], Mingjue Zhang[b], Wendao Wu[c], Wei Sun[c]

[a]*School of Chemistry and Chemical Engineering, Southeast University, Nanjing – 211189, China, email: 1543107327@qq.com (J. Li), Tel. +86-25-52090617, Fax +86-25-52090617, email: ymzhou@seu.edu.cn (Y. Zhou), 101006377@seu.edu.cn (Q. Yao), xywangtiantian77@163.com (T. Wang), 807543700@qq.com (A. Zhang), 838331357@qq.com (Y. Chen)*
[b]*School of Chemistry and Chemical Engineering, Southeast University Chengxian College, Nanjing – 211189, China, 53212651@qq.com (Q. Nan), 489354839@qq.com (M. Zhang)*
[c]*Jianghai Environmental Protection Co., Ltd., Changzhou, Jiangsu – 213116, China, email: 13887303@qq.com (W. Wu), leojhhg@sina.com (W. Sun)*

Received 12 January 2017; Accepted 9 August 2017

ABSTRACT

A kind of polyether-based copolymer, AA-TPEO, was synthesized using isoamyl alcohol polyoxyethylene ether, oxalic acid and acrylic acid. In this article, AA-TPEO was prepared at different mole ratios. After that, the synthesized polymer was characterized by Fourier-transform infrared (FT-IR) firstly. And further verification was done through ^{1}H NMR. Then, the molecular weight and its distributed situation were investigated by GPC. All of above consequences demonstrated that the synthetic experiment was successful. This work mainly aimed at investigating the impact of AA-TPEO's mole ratios and the agent concentration on scale inhibition efficiency of the copolymer for $CaSO_4 \cdot 2H_2O$ and $CaCO_3$ scales. From the results of the static scale inhibition experiments, it was known that AA-TPEO was a kind of efficient scale inhibitor. At the same time, its performance was compared with different inhibitors which were common on the market under the same conditions. The morphology and structure of deposits was confirmed by SEM, XRD and FT-IR. From the SEM photos, it could be seen that the surface appearance of $CaSO_4 \cdot 2H_2O$ and $CaCO_3$ scales changed. The lattice of $CaCO_3$ scales changed as the addition of AA-TPEO. The proposed inhibition mechanism of the copolymer was also described and analyzed briefly in this work.

Keywords: Calcium carbonate; Calcium sulfate dihydrate; Non-phosphorus; Polymer; Scale inhibitors

1. Introduction

As the need of providing economical heat removal and cost reductions, open recirculating cooling water systems are frequently used. One of the protruding problems of water cooling systems is scaling phenomenon, which has a great impact on economy and technology. Formation of deposit may cause deteriorated conditions of low heat exchange efficiency, and increase frequency of chemical cleaning [1–4]. What's more, massive precipitation of insoluble salts accumulated to some extent facilitates the corrosion processes, and even causes catastrophic operational failures in some cases, resulting in that production has to be stopped occasionally [5,6]. Commonly, the deposits are calcium carbonate ($CaCO_3$), calcium sulfate dihydrate ($CaSO_4 \cdot 2H_2O$), barium sulfate ($BaSO_4$), calcium phosphate ($Ca_3(PO_4)_2$), calcium oxalate, magnesium silicate [2,7–9], among which calcium sulfate dihydrate and calcium carbonate are considered most frequent in cooling water systems [2,9]. To mitigate or eliminate these problems, water used in cooling systems is treated with inhibitors which are water-soluble

*Corresponding author.

salts or polymers containing functional groups, affecting the nucleation rate, crystal growth, precipitated type, and crystal habit. The most effective groups are phosphonyl, carboxyl and sulfonyl [10–12]. Several studies about scales formation with and without inhibitors have been carried out [1,13].

In general terms, inhibitors are classified as inorganic salts and organic polymer compounds. Inorganic scale inhibitors, such as sodium hexametaphosphate, are used initially. Polyphosphates, organophosphonate (such as HEDP, 1-hydroxyethylidine 1,1-diphosphonic acid), and NTMP (nitrilo trimethylene phosphonate) [14–18], which are remarkable to chelate calcium ions, are major organic inhibitors in current recycling water systems. But these sorts of scale inhibitors are likely to accelerate water eutrophication [19,20], destroy the balance of ecological environment and cause water pollution. As a result, the popularity of inhibitor containing phosphorus is restricted. Consequently, searching for friendly ''green'' inhibitors is current trend.

As a kind of non-phosphorus inhibitor, polyether-based polymer was reported as polycarboxylate antiscalant for deposits, such as allylpolyethoxy carboxylate (APEC) reported by Du [21] and ammonium allylpolyethoxy sulfate (APES) reported by Steckler [22]. Both APEC and APES have carboxylic acid groups (–COOH), which can chelate Ca^{2+}, inhibiting the form of scales. However, chloracetic acid and sulfamic acid, used during the synthesis of APEC and APES, are harmful to water.

In response to the need of times, new inhibitor (AA-TPEO) was synthesized, using acrylic acid (AA), oxalic acid, and Methyl alkenyl polyoxyethylene ether (TPEG), which was a kind of double-hydrophilic block copolymer. Molecules of the copolymer contain many functional groups such as carbonyl, allyloxy, and ester, which bring the new inhibitor a number of advantages, for example, low material costs, simple experimental methods, high reaction ability, friendly to environment and high inhibition efficiency. Especially, no antiscalant for cooling water system that based on TPEG is reported in the literatures. The principal aim of this work is to investigate the performance of a structurally well-defined scale inhibitor which is phosphorus-free and has a superior calcium tolerance.

2. Experimental

2.1. Materials and instruments

TPEO and AA-TPEO were synthesized from Methyl alkenyl polyoxyethylene ether (TPEG), AA and Oxalic in our laboratory according to K. Du's procedure [21]. Calcium chloride, sodium bicarbonate, AA, sodium sulfate, and ammonium persulfate used during the experiment processes were obtained from Zhongdong Chemical Reagent Co., Ltd (Nanjing, Jiangsu, People's Republic of China). All the chemicals mentioned were in analytically pure grade need no further purification, unless otherwise specified. Commercial inhibitor, for instance, HPMA (Hydrolytic polymaleic anhydride MW = 600), PESA (polyepoxysuccinic acid MW = 1,500), PAA (Polyacrylic Acid, MW = 1800) and HEDP (Hydroxyethylidense-1, 1-diphosphonic acid MW = 206) were in technical pure grade and supplied by Jiangsu Jianghai Chemical Co., Ltd. Distilled water was used throughout this work.

The FT-IR spectra was recorded to verify the functional groups of the synthesized polymer that were responsible for the anti scaling property using a Bruker FT-IR analyzer (VECTOR-22, Bruker Co., Germany) in the pressed KBr slice. ^{1}H NMR spectra were given by a Mercury VX-500 spectrometer (Bruker AMX500) with a tetramethylsilane internal reference and deuterated dimethyl sulfoxide as the solvent. The MWs and MW polydispersities were measured using Gel permeation chromatography (GPC; Waters-2410, calibrated with PEG standards). Water was eluent flowing at a rate of 1.0 mL/min. The morphology of $CaSO_4$ $2H_2O$ and $CaCO_3$ were observed via scanning electron microscopy (SEM; S-3400 N, HITECH, Japan). The X-ray diffraction (XRD) studies were carried out to determine the crystal lattice of $CaSO_4$ $2H_2O$ and $CaCO_3$ using a Rigaku D/max 2400 X-ray powder diffractometer with Cu $K\alpha$ radiation (λ = 1.5406, 40 kV, 120 mA). The transform of the crystal form of $CaSO_4$ $2H_2O$ and $CaCO_3$ was also validated by FT-IR.

2.2. Preparation of TPEO and AA-TPEO

The terminal hydroxyl groups are carboxylic acid functionalized, realized with oxalic acid. The preparation procedure of TPEO is shown in Fig. 1.

AA-TPEO was synthesized in a five-neck round-bottom flask, equipped with a thermometer, a mechanical stirrer and reflux condenser, Firstly, the flask was charged with 80 mL distilled water and 0.1 mol TPEO which was heated to 60°C with stirring under nitrogen atmosphere. Secondly, 1.5 mol AA was added in 25 mL distilled water (the mole ratio of TPEO and AA was 1:15). Thirdly, the AA solution and the initiator solution (3.5 g ammonium persulfate in 25 mL distilled water) were added separately at constant flow rates over a period of 1.0 h. Finally, the reaction was heated to 90°C and maintained at this temperature for an additional

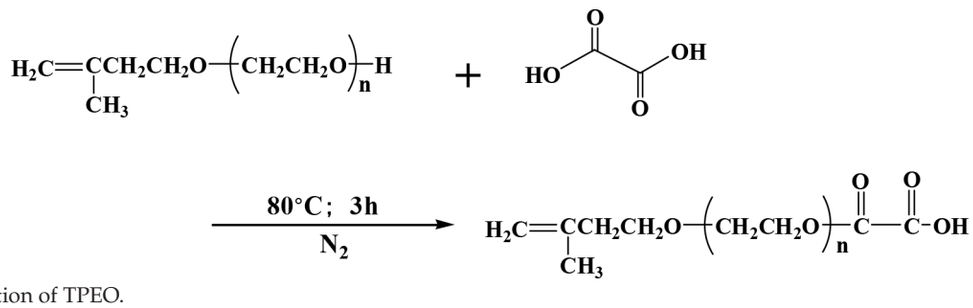

Fig. 1. Preparation of TPEO.

2 h. After above processes, an aqueous polymer solution containing approximately 24.3% effective component was obtained that was the product of AA-TPEO. The preparation procedure of AA-TPEO is shown in Fig. 2.

2.3. Inhibition test

The efficiency of the AA-TPEO inhibiting calcium sulfate dihydrate scale was compared with the ones which had no inhibitor in flask tests [23]. The inhibitor dosages given were according to dry basis. Precipitating process of calcium sulfate dihydrate and the inhibition performance of AA-TPEO were studied in artificial cooling water which was prepared by dissolving a certain quantity of $CaCl_2$ and Na_2SO_4 in distilled water. $CaC1_2$ solution (6,800 mg/L Ca^{2+}) and Na_2SO_4 solution (7,100 mg/L SO_4^{2-}) were used according to the national standard of China concerning the code for the design of industrial oilfield-water treatment (SY/T 5673–93). The supersaturated solutions containing different concentration of the copolymer was thermostated at 60°C for 10 h, whose pH was 7. The copolymer which was phosphorous free and non nitrogen had been synthesized in the laboratory before the test.

Solution was naturally cooled when the experiment was over and analyzed with respect to soluble calcium ions, titrated by a standard solution of EDTA according to standard methods (Water Treatment Reagent Unit of Standardization Research Institute of Chemical Industry of China 2003). We can calculate the inhibition efficiency follow the nether equation [24]:

$$\mu = \frac{\rho 1\left(Ca^{2+}\right) - \rho 2\left(Ca^{2+}\right)}{\rho 0\left(Ca^{2+}\right) - \rho 2\left(Ca^{2+}\right)} \times 100\% \quad (1)$$

where ρ0(Ca^{2+}) is the total concentrations of Ca^{2+} (mg/L), ρ1 (Ca^{2+}) is the concentrations of Ca^{2+} (mg/L) in the presence of the AA-TPEO copolymer, and ρ2(Ca^{2+}) is the concentrations of Ca^{2+}(mg/L) in the absence of the AA-TPEO copolymer.

Calcium carbonate inhibition test was alike to calcium sulfate dihydrate precipitation experiments according to the national standard of China concerning the code for the design of industrial circulating cooling-water treatment (GB/T 16632-2008). The supersaturated solutions used in tests were different, which was prepared by dissolving a certain concentration of $CaCl_2$ and $NaHCO_3$ in distilled water, not Na_2SO_4. And the concentrations of Ca^{2+} and HCO_3^- were 240 mg/L and 732 mg/L, respectively. The supersaturated solutions containing different quantities of the copolymer was thermostated at 80°C for 10 h, whose pH was 9. Calcium chloride and sodium bicarbonate used to prepare the scaling test solutions were of analytical reagent grade. The inhibition efficiency of AA-TPEO against calcium sulfate dihydrate scale was calculated as Eq. (1).

3. Results and discussion

3.1. Analysis of the copolymer

Fig. 3 exhibits the FT-IR spectra of TPEG (a), TPEO (b), and AA-TPEO (c). Compared with curve (a), the emerging 1,731 cm^{-1} strong intensity absorption peak (–C=O) in

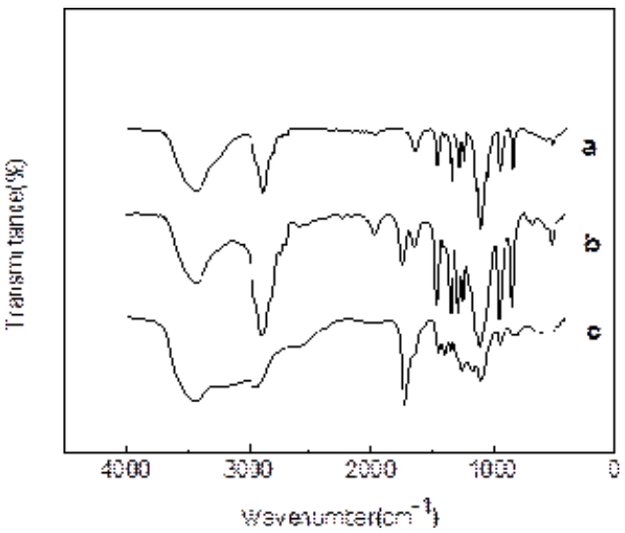

Fig. 3. The FT-IR spectra of (a) TPEG (b) TPEO and (c) AA-TPEO.

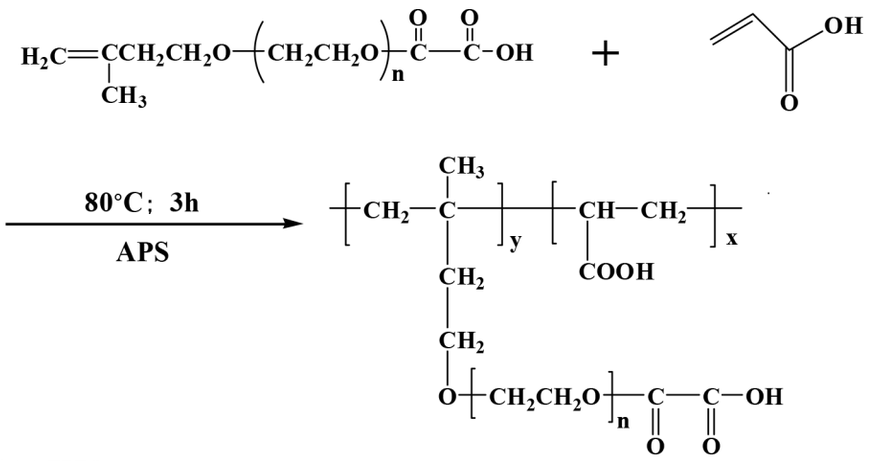

Fig. 2. Preparation of AA-TPEO.

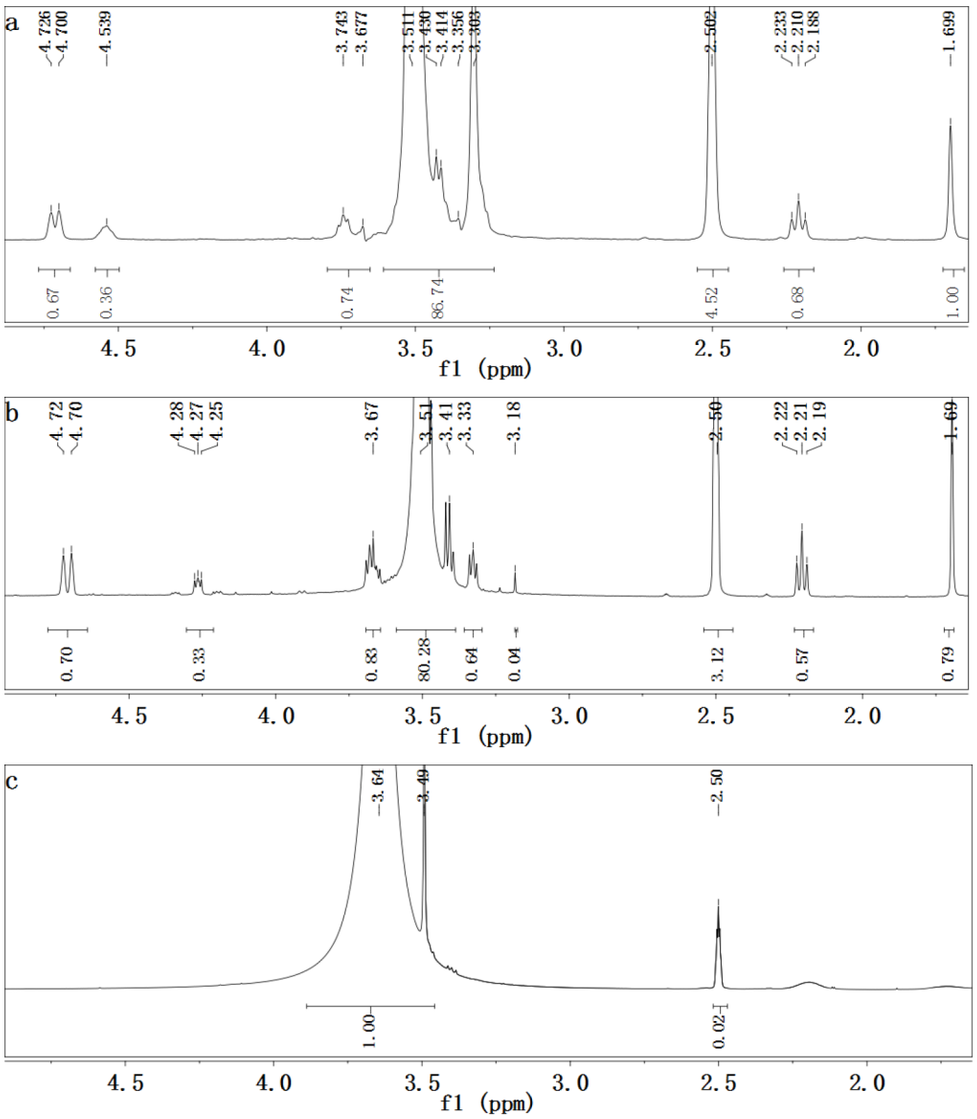

Fig. 4. The 1H NMR spectra of (a) TPEG, (b) TPEO, and (c) AA-TPEO.

curve (b) reveals clearly that TPEO has been synthesized successfully. The peak at 1,648 cm^{-1} are from the stretching of –C=C– groups, which appears in (a) and (b) but disappears in *c*. On the basis of FT-IR studies, the phenomenon reveals that the free radical polymerization between TPEO and AA has happened.

^{1}H NMR spectra for (a) TPEG, (b) TPEO and (c) AA-TPEO are shown in Fig. 4. TPEG (Fig. 4(a))($(CD_3)_2SO$, δ ppm): 2.50 (solvent residual peak of $(CD_3)_2SO$); 3.30–3.80 (–OCH_2CH_2–, ether groups); 1.69–1.70, 4.70–4.80 (CH_2 $C(CH_3)$–, methyl alkenyl); 4.40–4.60 (–OH, active hydrogen in TPEG).

TPEO (Fig. 4b) ($(CD_3)_2SO$, δ ppm): 2.50 (solvent residual peak of $(CD_3)_2SO$), 3.10–3.70 (–OCH_2CH_2–, ether groups). As the reaction between oxalic acid and TPEG is successful, –COCOOH affects the four hydrogen in –OCH_2CH_2– group which is near –COCOOH group; and 1.69–1.70, 4.20–4.80 (CH_2=$C(CH_3)$–, methyl alkenyl). As seen, the δ 4.40–4.60 ppm (–OH) active hydrogen in (a) disappears completely, proving that –OH in TPEG has been entirely replaced by –COCOOH.

AA-TPEO (Fig. 4c) ($(CD_3)_2SO$, δ ppm): 2.50 (solvent residual peak of $(CD_3)_2SO$), The phenomenon, that δ1.69–1.70, 4.20–4.80 ppm in (b) double bond absorption peaks completely disappear in (c), reveals that free radical polymerization between TPEO and AA has happened. From the analysis of FT-IR and ^{1}H NMR, it can be concluded that synthesized AA-TPEO has anticipated structure.

The molecular weight was an important parameter of inhibitor, which was investigated through GPC (calibrated with PEG standards) with the 1.0 mL/min run flow rate and the results are listed in Table 1.

3.2. Effect of inhibitor on scales

Monomer's mole ratio and dosage of scale inhibitor greatly influence performances of AA-TPEO. Table 2 and

Table 1
Molecular weight averages of the polymer

Mp	12,770
Mn	7,796
Mw	10,897
Mz	14,288
Mz+1	17,373
Mv	10,410
PDI	1.3977

Table 3 show the relationship between the inhibitor dosage and the inhibition efficiency towards $CaSO_4{\cdot}2H_2O$ and $CaCO_3$ scales for different mole ratios. It is observed that the scale inhibition efficiency improves as the concentration of the copolymer increases. Fig. 5 exhibits that, when the dosage is only 5 ppm, the maximum inhibition efficiency reach 100%, better than the majority of no-phosphorus inhibitors on the market for $CaSO_4{\cdot}2H_2O$ [25]. But the increasing trend of the inhibition efficiency dies down with the gradually increasing concentration. Obviously, from Fig. 6, when the dosage is 10 ppm (= 10 mg/L), AA-TPEO has a goodish calcium tolerance, with 86% $CaCO_3$ inhibition efficiency. The efficiency improves to 89% as the concentration increases to 12 ppm. However, the performance declines more or less as the concentration further increases as the concentration further increases. The copolymer has ability of positive dispersion, excellent chelation, superior compatibilization with calcium ions and lattice distortion. The molecules' chains contain carboxylate (–COOH) and ethylnenoxy ($–OCH_2CH_2–$) groups. It is those active functional groups that possess great properties inhibiting scales. As mentioned above, for the same scale inhibitor, the scale inhibitive performance of the polymer improves as the concentration gradually increases, as interaction between the scale inhibitor and Calcium ions becomes stronger. When copolymer AA-TPEO is at the dosage of 4 ppm and 10 ppm, the inhibition efficiency is 99% and 86% for $CaSO_4{\cdot}2H_2O$ and $CaCO_3$, respectively. However, when the amount of polymer is excessive, the flocculation phenomenon appears, due to strong polar interaction of active groups on the molecular chain, which leads to decline of the performance of inhibitor AA-TPEO slightly for $CaSO_4{\cdot}2H_2O$ and $CaCO_3$. It's found that at the same concentration level of AA-TPEO, inhibition efficiency towards $CaSO_4{\cdot}2H_2O$ and $CaCO_3$ scales are all the highest when the mole ratio is 2:1(AA: TPEO) among the different ratios.

3.3. Comparisons of inhibition efficiency

Fig. 5 illustrates the ability of different inhibitors controlling calcium sulfate dihydrate precipitation, that is AA-TPEO, HEDP (1-hydroxyethylidine 1, 1-diphos-phonic

Table 2
Influence of the dosage and monomer's mole ratio of AA-TPEO on the inhibition efficiency of $CaSO_4$

Dosage of inhibitor (ppm)	1:3	1:2	1:1	2:1	3:1	4:1	5:1
1	9.42	23.79	16.91	51.06	34.38	3.99	18.00
2	23.91	29.11	22.93	77.17	49.13	22.10	22.10
3	50.99	49.49	50.84	96.30	60.51	53.33	40.82
4	71.20	67.44	68.72	99.85	80.33	75.65	64.51
5	84.44	81.06	82.66	100	94.30	83.90	76.79
7	96.52	92.17	95.56	100	94.29	93.33	92.34
w	93.43	91.38	92.50	100	100	100	97.83

Table 3
Influence of the dosage and monomer's mole ratio of AA-TPEO on the inhibition efficiency of $CaCO_3$

Dosage of inhibitor (ppm)	1:3	1:2	1:1	2:1	3:1	4:1	5:1
4	4.76	14.29	29.05	53.35	45.00	24.76	43.81
5	9.52	28.57	47.62	55.15	50.03	28.57	52.67
6	9.52	28.57	50.95	58.65	52.63	38.10	56.57
7	14.29	37.14	55.00	62.34	55.26	39.29	57.14
8	19.05	39.14	64.29	66.29	59.53	47.39	57.62
9	19.05	42.86	64.29	76.90	61.89	58.57	64.29
10	19.05	44.35	65.34	86.58	61.98	60.79	67.27
12	19.05	47.62	66.90	89.43	63.16	64.76	70.06
15	19.05	52.38	71.43	87.05	63.16	66.67	69.52

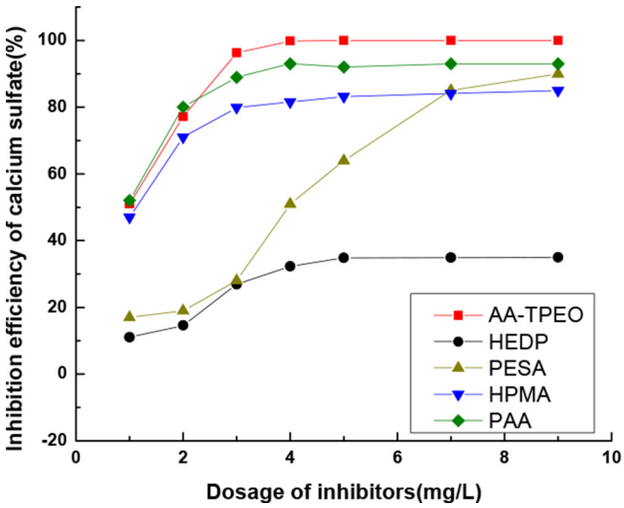

Fig. 5. Comparison of inhibition efficiency for $CaSO_4$.

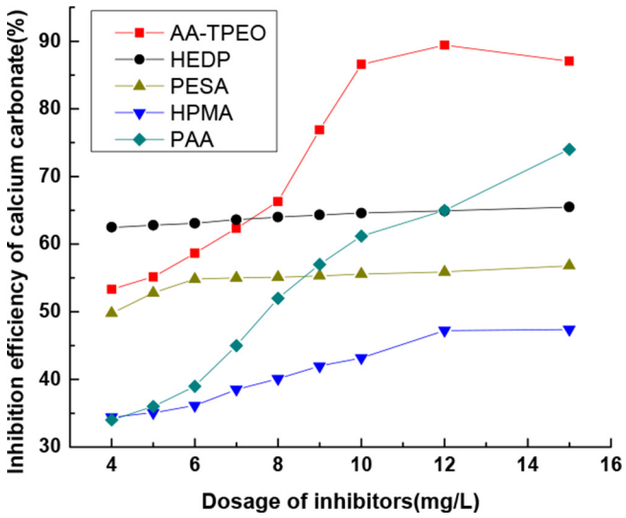

Fig. 6. Comparison of inhibition efficiency for $CaCO_3$.

acid), PESA (poly(epoxysuccinic acid)), PAA(Polyacrylic Acid) and HPMA (hydrolytic poly(maleic anhydride)), low-phosphorus or non-phosphorus polymers. All the curves in Fig. 5 show that the ability to inhibit calcium sulfate dihydrate precipitation follows the order AA-TPEO > PAA > HPMA > PESA (at low dosage) > HEDP. From Fig. 5 we can see that inhibition on calcium sulfate dihydrate precipitation by the presence of PESA is little (4 mg/L only 82% calcium sulfate dihydrate inhibition). However, AA-TPEO shows high inhibition efficiency. Particularly, HPMA (56%) seems more effective than AA-TPEO (51%) for the calcium sulfate dihydrate inhibition at the level of 1 mg/L. But, when exceeding 3 mg/L, AA-TPEO (96%) shows much higher inhibition efficiency than HPMA (79%). Consequently, among inhibitors investigated, inhibitor AA-TPEO displays the best performance to control calcium sulfate dihydrate scale, namely, better than HEDP, HPMA, PAA and PESA.

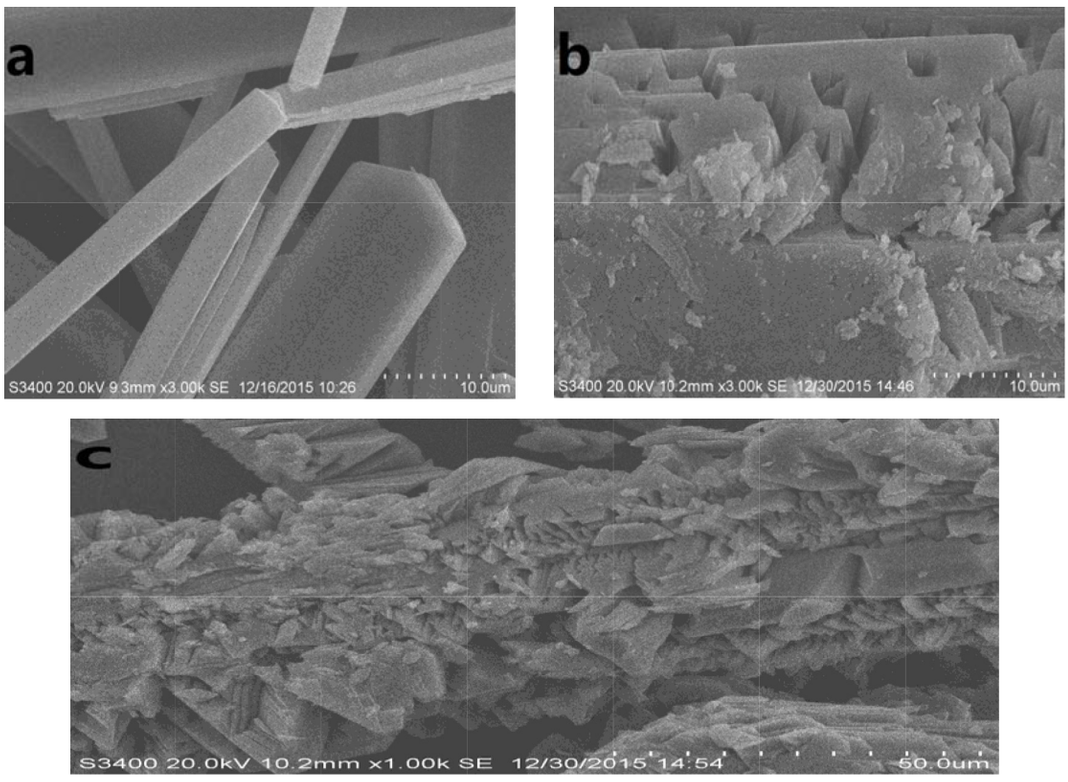

Fig. 7. SEM images for the calcium sulfate (a) without AA-TPEO (b) with 1 mg/L AA-TPEO (c) with 3 mg/L AA-TPEO.

From Fig. 6 we can see that the performance of AA-TPEO preventing the precipitation of $CaCO_3$ is the best. It must be mentioned that HEDP has an advantage in the threshold dosage as $CaCO_3$ antiscalant, which is only 4 mg/L less than 10 mg/L for AA-TPEO, although HEDP has only 65% calcium carbonate inhibition efficiency while the inhibition efficiency of AA-TPEO could reach 89% at the threshold dosage.

3.4. Scale surface morphology characterization

SEM, one of the popular nondestructive surface examination techniques was used to examine the change of crystal size and modifications, brought about by the addition of AA-TPEO copolymer.

The SEM images of calcium sulfate dihydrate precipitate form in simulative cooling water are shown in Fig. 7. We can see that the application of the copolymer in the system (Fig. 7b,c) is an effective way to transform the morphology of the calcium sulfate dihydrate. Without inhibitor, regular rod-shaped calcium sulfate dihydrate scale is obtained (Fig. 7a), which look like thin tubular cells and needles exhibiting monoclinic symmetry [9]. In the presence of 1 mg/L AA-TPEO, the morphology of the scale changes and the loose calcium sulfate dihydrate particles appear (Fig. 6b). When the AA-TPEO concentration soars to 3 mg/L, the loose particles become the major part of the calcium sulfate dihydrate scale. And when 4 mg/L is used, the scale is hard to be observed, in accordance to the inhibition of 99% mentioned above. After the inhibition period, the morphology of $CaSO_4$ $2H_2O$ changes drastically.

The morphology images of the $CaCO_3$ deposits obtained with no and 4, 7, 10 mg/L (ppm) antiscalant are exhibited in Fig. 8. As we can see from Fig. 8a, calcium carbonate scales are mainly calcite scales, which are symmetrical and block like particles of cubic shape or rhombohedral. Changes of the calcite crystal morphology and the crystal size could be observed from Fig. 8b–d, in the presence of the non-phosphorus copolymer AA–TPEO. Fig. 8b, obtained at the dosage of 4 ppm, exhibits that the well-regulated structure is modified. The deposition transform into smaller crystals and the shape edges disappeared. As shown in Fig. 8c, when 7 ppm inhibitor is used, the crystal turn into slices, which are loose and porous. With 10 ppm inhibitor addition, the scales are damaged absolutely, which nearly become fragments.

All variations above manifest that the copolymer affects the nucleation and morphology of $CaCO_3$ precipitate, and the influence intensify as the concentration of the AA-TPEO increase.

3.5. XRD analysis of $CaSO_4$ $2H_2O$ and $CaCO_3$ crystals

To verify the structural changes of calcium sulfate dihydrate and calcium carbonate deposits in the absence and presence of the inhibitor, XRD analysis was carried out.

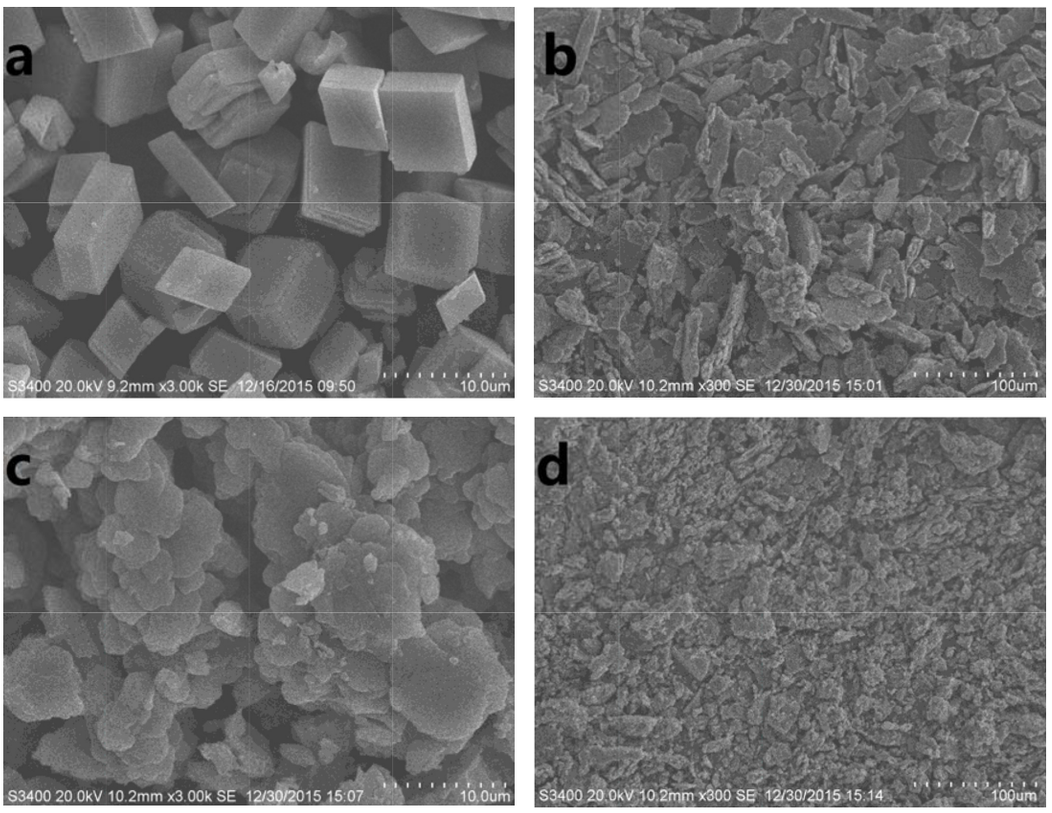

Fig. 8. SEM images for the calcium carbonate (a) with no inhibitor (b) with 4 mg/L AA-TPEO (c) with 7 mg/L AA-TPEO (d) with 10 mg/L AA-TPEO.

Figs. 9 and 10 show the XRD spectra of calcium sulfate dihydrate crystals without and with the addition of the AA-TPEO copolymer. In the spectrogram, the θ values conform to the structure of $CaSO_4{\cdot}2H_2O$ (calcium sulfate dihydrate) [26,27]. During the tests, the copolymer added does not alter the crystal structure, which confirmed by no variations in its θ values. Only the crystal morphology is modified, as shown in the SEM photographs.

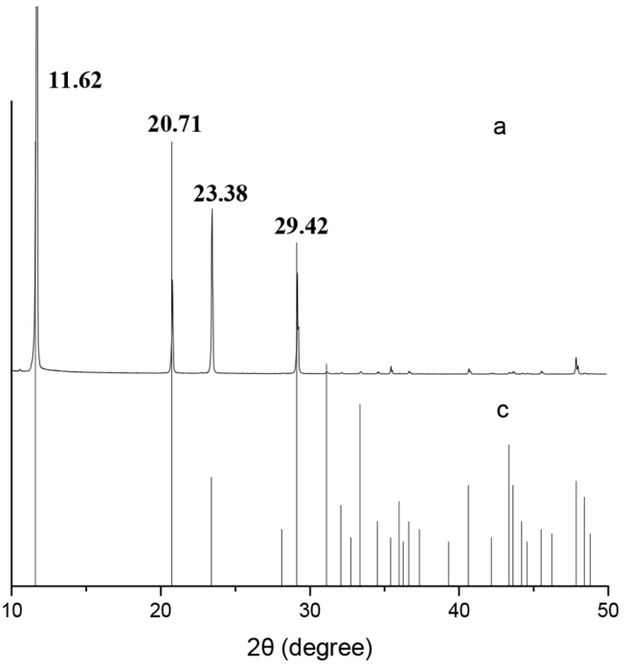

Fig. 9. XRD spectrum for $CaSO_4{\cdot}2H_2O$: (a) with no AA-TPEO (c) the reference pattern for $CaSO_4{\cdot}2H_2O$.

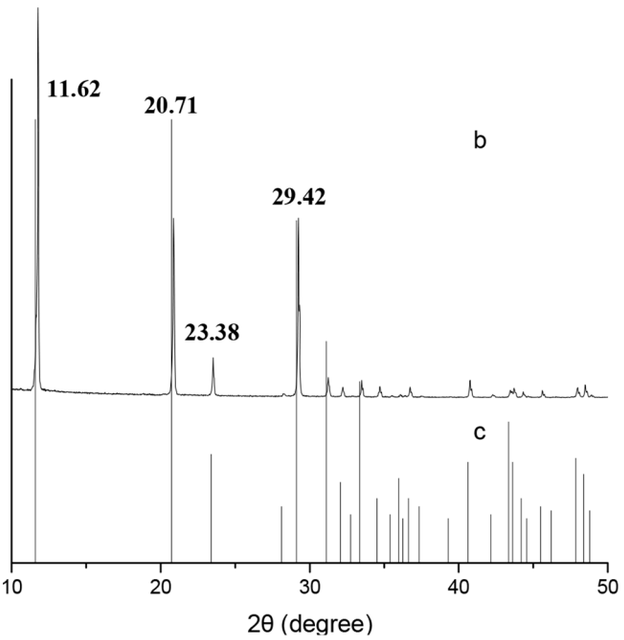

Fig. 10. XRD spectrum for $CaSO_4{\cdot}2H_2O$: (b) with AA-TPEO (c) the reference pattern for $CaSO_4{\cdot}2H_2O$.

In nature, $CaCO_3$ crystal has three types of forms: calcite, aragonite, and vaterite, in which calcite is the most thermodynamically stable and vaterite is the least stable form. In untreated supersaturated solutions, as exhibited in Fig. 11a, $CaCO_3$ deposits crystallize as prismatic calcite. And its diffraction peaks appear at 012, 104, 006, 110, 113, 202, 018, and 116.As antiscalant is used, in Fig. 11b, peaks appear at 110, 112,114, and 300 corresponding to vaterite in addition to the calcite peaks [3]. The results manifest that calcium carbonate would first nucleate and deposit as calcite and then convert to an unstable form (vaterite) after adding AA-TPEO [3].

3.6. FT-IR analysis of $CaCO_3$ crystals

FT-IR, as another characterization technique to identify the form changes of the crystals, was carried out. Fig. 12 exhibits the FT-IR spectra of the calcium carbonate precipitates obtained in the absence and presence of the copolymer. We can see from curve (a) that the peaks appear at 874 and 712 cm^{-1} ,which are assigned to the vibrations of calcite [28]. From curve (b), we find that peak at 712 cm^{-1} disappears, while a new peak at 745 cm^{-1} emerges, which symbolises the vaterite form. All the variation of the FT-IR spectra demonstrate that the copolymer influences the polymorph of the calcium carbonate crystals.

4. Inhibition mechanism towards $CaSO_4$ $2H_2O$ and $CaCO_3$

Generally speaking, it's the location of the adsorbed inhibitor at the crystal surface and the extent of chemical

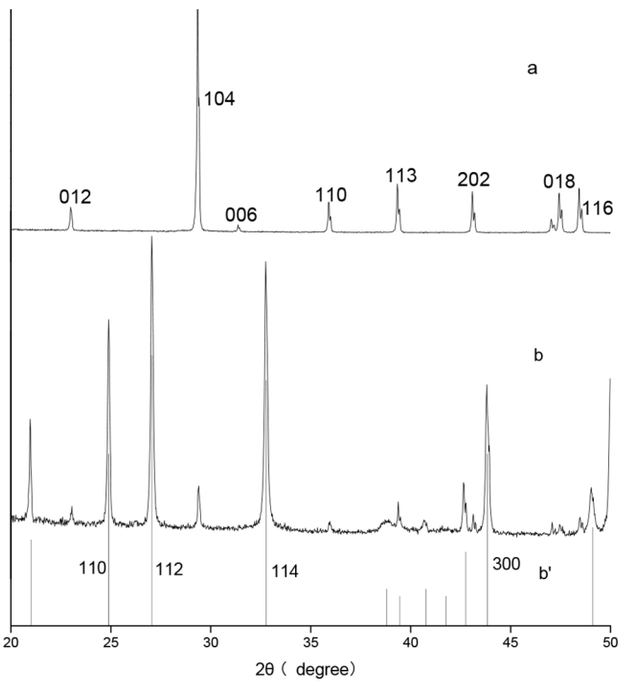

Fig. 11. XRD spectrum for calcium carbonate: (a) in absence of AA-TPEO (b) in presence of AA-TPEO (b′) the reference pattern for vaterite.

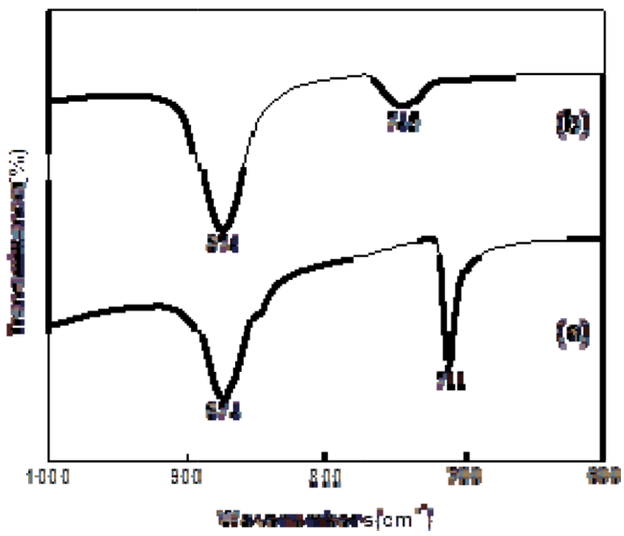

Fig. 12. FT-IR spectra of $CaCO_3$ precipitate (a) In the absence of AA-TPEO (b) in the presence of AA-TPEO.

bonding with the surface that influence the control of the formation of scale, and the functional groups of inhibitor play a significant role in terms of controlling the scale precipitation [29]. The AA-TPEO copolymer contains a large number of carboxyl groups, and carboxyl segments as well as $(CH_2CH_2O)_n$ groups are main functional parts of AA-TPEO, Which makes the inhibitor's surface-binding capability is strong and inhibition efficiency is high.

From Fig. 13 we can see that the main chains consist of allyl-terminated AA, PAA for short, and the side chains are composed of $(CH_2CH_2O)_n$ segments. As we know, $(CH_2CH_2O)_n$ segments are hydrophilic blocks. PAA can discern and chelate with calcium ions on the surface of inorganic minerals, such as calcium sulfate dihydrate and calcium carbonate deposits (Fig. 8b), weakening the activity of free Ca^{2+} and reducing the degree of supersaturation. AA-TPEO-COOCa complexes form after interaction between calcium ions and part of carboxyl groups. Meanwhile, $(CH_2CH_2O)_n$ segments exert strong hydrophilicity. Thus, solid particles such as $CaCO_3$ scales and $CaSO_4{\cdot}2H_2O$ scales could be dispersed and exist in water stably. In short, mechanism 1 shown in Fig. 13 is chelating and solubilization. The other carboxyl groups take part in crystallization process while chelating with calcium ions on the surface of inorganic minerals, which makes the deposits' lattice unnormal, as shown in Fig. 14. Consequently, the deposits are loose, less prone to further growth, hard to adhere on walls and easy to be washed away [30]. All above indicate that AA-TPEO possesses excellent ability to control $CaSO_4$ $2H_2O$ and $CaCO_3$ scale.

5. Conclusions

Through experiments, the copolymer AA–TPEO has been synthesized successfully, and characterized by FTIR, ^{1}H-NMR. Its performance is evaluated via static scale inhibition method. From foregoing contents, we have the nether conclusions:

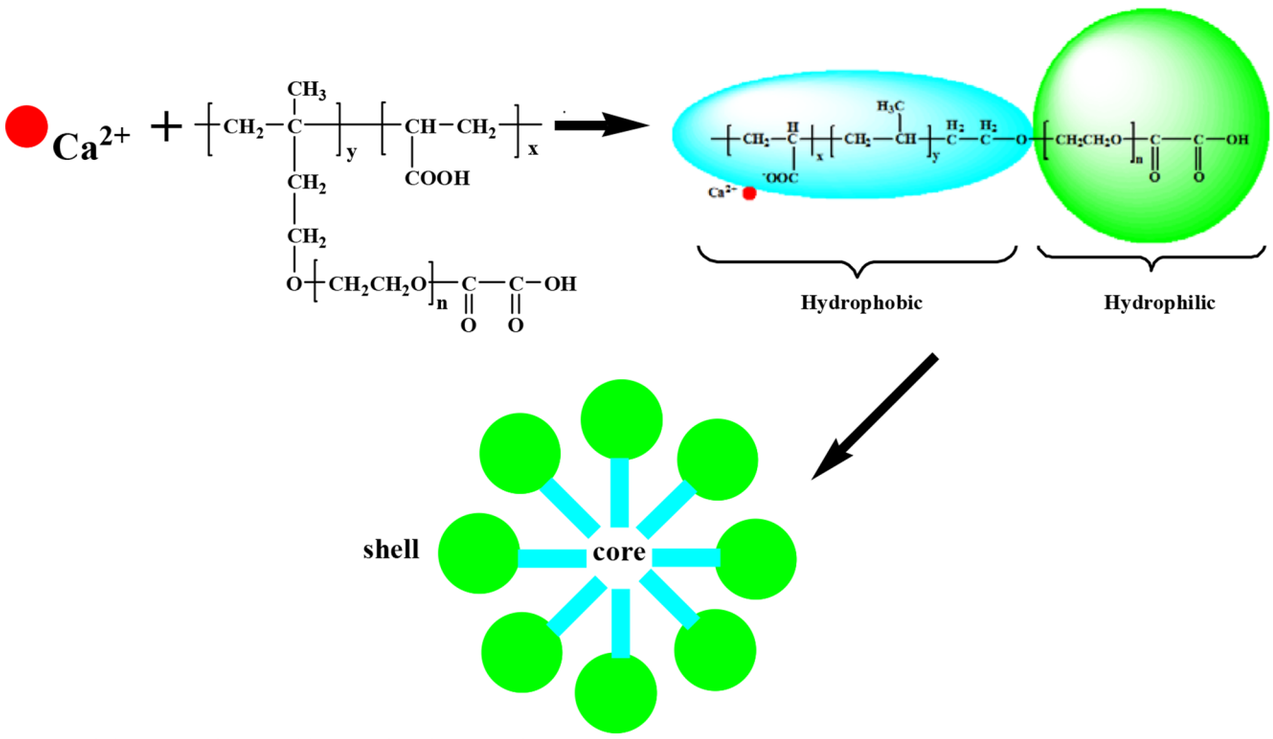

Fig.13. Inhibition mechanism (1) towards calcium scale.

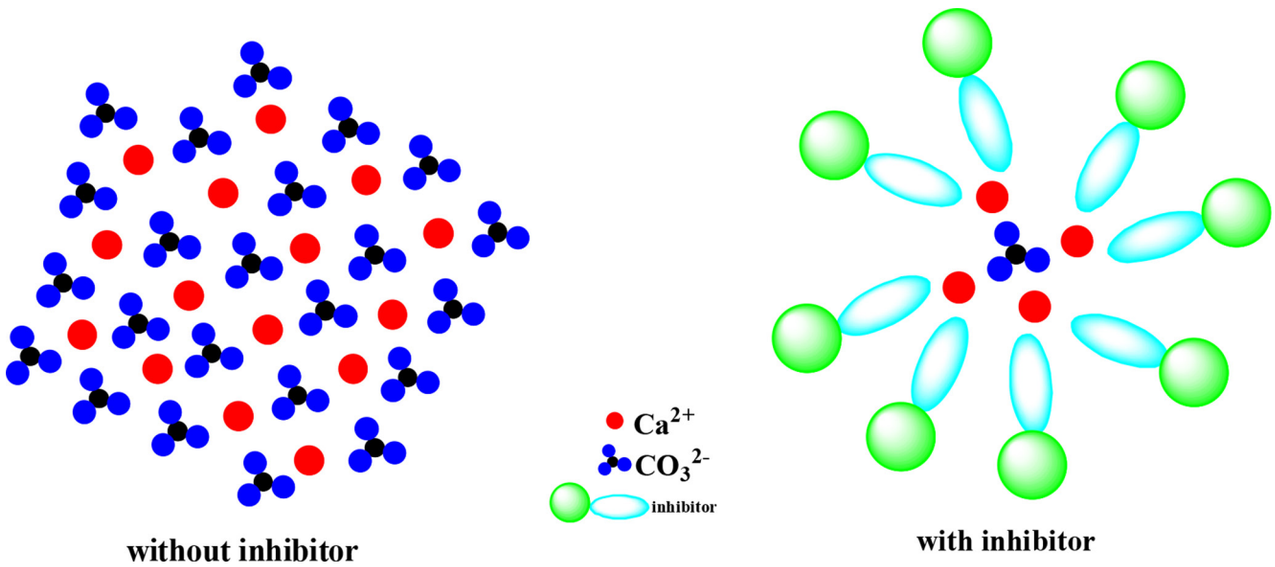

Fig. 14. Inhibition mechanism (2) towards calcium scale.

AA-TPEO can inhibit formation of $CaSO_4 \cdot 2H_2O$ deposits primely. Its inhibition efficiency is 100% at about 4 ppm.

The $CaCO_3$ inhibition efficiency of AA-TPEO is investigated, which decreases in the following order: 2:1 (AA:TPEO, mole ratio) > 5:1 > 1:1 > 4:1 > 3:1 > 1:2 > 1:3. When the dosage is 12 ppm, inhibition efficiency is 89.43%.

Compared with the inhibitor commercially available, such as HEDP, PESA, PAA and HPMA, AA-TPEO has superior scale inhibition performance.

The studies on calcium crystals with SEM, XRD, and FT-IR have been carried out, which demonstrate that, under the influence of AA–TPEO, great changes in the size and morphology of the scales have taken place.

The inhibition mechanism of TPEO controlling $CaCO_3$ and $CaSO_4 \cdot 2H_2O$ deposits is proposed that encapsulation or interaction happens between PAA fragment and Ca^{2+}, which forms the core–shell structure increasing solubility of the inorganic minerals. Meanwhile, the copolymers take part in crystallization processes of the scale, altering the lattice, restraining the further growth of the crystal nuclear, which makes the deposits loose and little. Thus, the scales are hard to adhere to the equipments and easy to be washed away.

These results indicate that AA-TPEO is a potentially green inhibitor for circulating cooling water.

This work is supported by the National Natural Science Foundation of China (51673040); a Project Funded by the Priority Academic Program Development of Jiangsu Higher Education Institutions (PAPD) (1107047002); The Fundamental Research Funds for the Central Universities (3207046302); the Prospective Joint Research Project of Jiangsu Province (BY2016076-01); Scientific Innovation Research Foundation of College Graduate in Jiangsu Province (KYLX16_0266); Fund Project for Transformation of Scientific and Technological Achievements of Jiangsu Province of China (BA2016105); and Based on Teachers' scientific research SRTP of southeast University (T16192003).

References

[1] D.E. Abd-El-Khalek, B.A. Abd-El-Nabey, Evaluation of sodium hexametaphosphate as scale and corrosion inhibitor in cooling water using electrochemical techniques, Desalination, 311 (2013) 227–233.

[2] A.L. Kavitha, T. Vasudevan, H.G. Prabu, Evaluation of synthesized antiscalants for cooling water system application, Desalination, 268 (2011) 38–45.

[3] C. Wang, S.P. Li, T.D. Li, Calcium carbonate inhibition by a phosphonate-terminated poly (maleic-co-sulfonate) polymeric inhibitor, Desalination, 249 (2009) 1–4.

[4] Z.H. Shen, J.S. Li, K. Xu, L.L. Ding, H.Q. Ren, The effect of synthesized hydrolyzed polymaleic anhydride (HPMA) on the crystal of calcium carbonate, Desalination, 284 (2012) 238–244.

[5] E. Barouda, K.D. Demadis, S.R. Freeman, F. Jones, M.I. Ogden, Barium Sulfate Crystallization in the Presence of Variable Chain Length Aminomethylenetetraphosphonates and Cations (Na^+ or Zn^{2+}), Cryst. Growth Des., 7 (2007) 321–327.

[6] F.M. Mahgoub, B.A. Abdel-Nabey, Y.A. El-Samadisy, Adopting a multipurpose inhibitor to control corrosion of ferrous alloys in cooling water systems, Mater. Chem. Phys., 120 (2010) 104–108.

[7] P. Shakkthivel, T. Vasudevan, Newly developed itaconic acid copolymers for gypsum and calcium carbonate scale control, J. Appl. Polym. Sci., 103 (2007) 3206–3213.

[8] M.B. Amor, D. Zgolli, M.M. Tlili, A.S. Manzola, Influence of water hardness, substrate nature and temperature on heterogeneous calcium carbonate nucleation, Desalination, 166 (2004) 79–84.

[9] P. Shakkthivel, T. Vasudevan, Acrylic acid-diphenylamine sulphonic acid copolymer threshold inhibitor for sulphate and carbonate scales in cooling water systems, Desalination, 197 (2006) 179–189.

[10] A. Sand, M. Yadav, K. Behari, Preparation and characterization of modified sodium carboxymethyl cellulose via free radical graft copolymerization of vinyl sulfonic acid in aqueous media, Carbohyd. Polym., 81 (2010) 97–103.

[11] Z.M. Wang, L. Li, K.J. Xiao, J.Y. Wu, Homogeneous sulfation of bagasse cellulose in an ionic liquid and anticoagulation activity, Bioresour. Technol, 100 (2009) 1687–1690.

[12] Z. Reddad, C. Gerente, Y. Andres, P.L. Cloirec, J.-F. Thibault, Cadmium and lead adsorption by a natural polysaccharide in MF membrane reactor: experimental analysis and modelling, Water Res., 37 (2003) 3983–3991.

[13] G. Maurin, C. Gabrielli, H. Perrot, G. Poindessous, R. Rosset, Investigation of electrochemical calcareous scaling Potentiostatic current - and mass-time transients, J. Electroanal Chem., 538–539 (2002) 133–143.
[14] K.D. Demadis, A. Ketsetzi, Degradation of Phosphonate - based scale inhibitor additives in the presence of oxidizing biocides: "collateral damages" in industrial water systems, Separ. Sci. Technol., 42 (2007) 1639–1649.
[15] J. Marín-Cruz, R. Cabrera-Sierra, M.A. Pech-Canul, I. González, EIS characterization of the evolution of calcium carbonate scaling in cooling systems in presence of inhibitors, J. Solid State Electrochem., 11 (2007) 1245–1252.
[16] P.J. Maite, L. Ye, Z.G. Yuan, Free nitrous acid inhibition on the aerobic metabolism of poly-phosphate accumulating organisms, Water Res., 44 (2010) 6063–6072.
[17] J.H. Guo, S.J. Severtson, Inhibition of Calcium Carbonate Nucleation with Aminophosphonates at High Temperature, pH and Ionic Strength, Ind. Eng. Chem. Res., 43 (2004) 5411–5417.
[18] S.J. Dyer, C.E. Anderson, G.M. Graham, Thermal stability of amine methyl phosphonate scale inhibitors, J. Petrol, Sci. Eng., 43 (2004) 259–270.
[19] Z. Amjad, Investigations on the evaluation of polymeric calcium sulfate dihydrate (gypsum) scale inhibitors in the presence of phosphonates, Desal. Water Treat., 37 (2012) 268–276.
[20] L. Boels, G.J. Witkamp, Carboxymethyl inulin biopolymers: a green alternative for phosphonate calcium carbonate growth inhibitors, Cryst Growth Des., 11 (2011) 4155–4165.
[21] K. Du, Y.M. Zhou, L.Q. Wang, Y.Y. Wang, Fluorescent-tagged no phosphate and nitrogen free calcium phosphate scale inhibitor for cooling water systems, J. Appl. Polym. Sci., 113 (2009) 1966–1974.
[22] K. Cao, Y.M. Zhou, G.Q. Liu, H.C. Wang, S. Wei., Preparation and properties of a polyether-based polycarboxylate as an antiscalant for gypsum, J. Appl. Polym. Sci., 131 (2014).
[23] G.Q. Liu, J.Y. Huang, Y.M. Zhou, Q.Z. Yao, L. Ling, P.X. Zhang, H.C. Wang, K. Cao, Y.H. Liu, W.D. Wu, W. Sun, Z.J. Hu, Fluorescent-tagged double-hydrophilic block copolymer as a green inhibitor for calcium carbonate scales, Tenside Surf. Coat. Technol., 5 (2012) 404–412.
[24] C.E. Fu, Y.M. Zhou, G.Q. Liu, J.Y. Huang, W. Sun, W. Wu, Inhibition of $Ca_3(PO_4)_2$, $CaCO_3$, and $CaSO_4$ precipitation for industrial recycling water, Ind. Eng. Chem. Res., 50 (2011) 10393–10399.
[25] H. Wang, G. Liu, J. Huang, Y. Zhou, Q. Yao, S. Ma, K. Cao, Y. Liu, W. Wu, W. Sun, Z. Hu, Performance of an environmentally friendly anti-scalant in $CaSO_4$ scale inhibition, Desal. Water Treat., 53 (2013) 8–14.
[26] H.A. E1 Dahan, H.S. Hegazy, Gypsum scale control by phosphate ester, Desalination, 127 (2000) 111–118.
[27] P. Shakkthivel, D. Ramesh, R. Sathiyamoorthi, T. Vasudevan, Water soluble copolymers for calcium carbonate and calcium sulphate scale control in cooling water systems, J. Appl. Polym. Sci., 96 (2005) 1451–1459.
[28] U. Norikazu, H. Tsutomu, Y. Yusuke, D. Mototsugu, O. Takaaki, N. Akira, Calcium Complexes of carboxylate-containing polyamide with sterically disposed NH,O hydrogen bond: detection of the polyamide in calcium carbonate by 13C cross-polarization/magic angle spinning spectra, Macromolecules, 31 (1998).
[29] C.E. Fu, Y.M. Zhou, H.T. Xie, W. Sun, W.D. Wu, Double-hydrophilic block copolymers as precipitation inhibitors for calcium phosphate and iron(III), Ind. Eng. Chem. Res., 49 (2010) 8920–8926.
[30] P. Huber, A. Burnet, M. Petit-Conil, Scale deposits in kraft pulp bleach plants with reduced water consumption: a review, J. Environ. Manage., 141 (2014) 36–50.